# Pairing of cation vacancies and gap-state creation in $TiO_2$ and $HfO_2$

Hyo-Shin Ahn and Seungwu HanCheol Seong Hwang

Citation: Appl. Phys. Lett. **90**, 252908 (2007); doi: 10.1063/1.2749858
View online: http://dx.doi.org/10.1063/1.2749858
View Table of Contents: http://aip.scitation.org/toc/apl/90/25
Published by the American Institute of Physics

# Pairing of cation vacancies and gap-state creation in $TiO_2$ and $HfO_2$

Hyo-Shin Ahn and Seungwu Han[a)]
*Department of Physics, Ewha Womans University, Seoul 120-750, Korea*

Cheol Seong Hwang
*School of Materials Science and Engineering, Seoul National University, Seoul 151-742, Korea*

(Received 26 March 2007; accepted 24 May 2007; published online 21 June 2007)

Based on the first-principles calculations, the authors study defect-defect interactions between cation vacancies in rutile $TiO_2$ and monoclinic $HfO_2$. It is found that vacancies are greatly stabilized at small separations because of a large reconstruction of nearby oxygen atoms that have two broken bonds. As a result, O–O bonds resembling $O_2$ or $O_3$ molecules are formed near the divacancy site. The defect levels originated from antibonding states of O *p* orbitals are identified within the energy gap, which can affect leakage currents and the density of trapped charges of oxides substantially.
 [DOI: 10.1063/1.2749858]

The transport properties of transition metal oxides used in microelectronic devices critically depend on the defect types present in the material. For example, defects are often a microscopic origin of leakage currents of dielectrics either by doping the material with carriers or creating in-gap states that can be involved in the trap-detrap process. The defects are generated from various sources during the growth/annealing procedures or in the middle of device operations. In many transition metal oxides, the predominant point defect is usually the oxygen vacancy.[1,2] Although defects with the opposite character, the cation vacancy, are created much less than oxygen vacancies under a typical growth condition, its presence could result in an electronic property distinct from the case of anion vacancies. One such example is a recent observation of the ferromagnetic signal in $HfO_2$.[3] It has been proposed that the ferromagnetic ordering could be induced around Hf vacancy sites.[4] Despite their importance, defect structures of cation vacancies and their influence on the electronic structure are rarely elaborated.

In this letter, we carry out first-principles studies on the cation vacancy in two representative *n*-type binary oxides, $TiO_2$ and $HfO_2$. $TiO_2$ is a candidate replacement dielectrics to be used in the capacitor component of the dynamic random access memory with gigabit densities, while $HfO_2$ is the base material of the high-*k* gate dielectrics in logic semiconductor devices, although Hf silicates or its oxynitrides are more favored to overcome the mobility degradation and Fermi-level pinning. In those oxides, various types of defects exist from the nonstoichiometric composition, especially for the low-temperature growth methods such as atomic layer deposition (ALD) often adopted to synthesize thin films of $TiO_2$ and $HfO_2$. For instance, it has been reported that $HfO_2$ grown by an ALD method using a metal-organic precursor and $O_3$ at a temperature of 300 °C have an oxygen-excessive composition (O/Hf atomic ratio of ~2.2–2.4).[5] The oxygen-excessive $TiO_2$ thin films were also grown by ALD using a metal-organic precursor and $O_3$ at a temperature of 250 °C (O/Ti atomic ratio of ~2.2)[6] and high-pressure reactive sputtering at a temperature of 200 °C (O/Ti atomic ratio of ~2.17).[7] In those oxygen-rich samples, the oxygen interstitial and cation vacancy can be considered as major point defects although specific defect structures and densities have not been verified experimentally. As is found in Ref. 2 and also confirmed in this work (see below), the oxygen interstitial has little effect on electronic structures. In addition, it might be easily removed through annealing processes. On the other hand, we find that the cation vacancies stabilized in the divacancy configuration give rise to defect levels in the energy gap that can increase leakage currents or the density of trapped charges.

We use Vienna *ab initio* simulation package (VASP) for the first-principles calculations.[8] The projector augmented wave pseudopotentials[9] are employed to describe the electron-ion interaction. The valence configurations are $4s^2 3d^2$, $[5p^6]5d^2 6s^2$, and $2s^2 2p^4$ for Ti, Hf, and O atoms, respectively. (The semicore states are bracketed.) The electron-electron interactions are described within the local density approximation.[10] For the case of $HfO_2$, we consider spin polarization to address finite magnetic moments. The energy cutoff is chosen to be 500 eV and the $4\times4\times6$ and $4\times4\times4$ Monkhorst-Pack grids are employed in the Brillouin zone integration for rutile $TiO_2$ and monoclinic $HfO_2$ unit cell, respectively. When supercells made of $3\times3\times5$ ($2\times2\times2$) repetitions of unit cells are used for studying defects in $TiO_2$ ($HfO_2$), $1\times1\times1$ ($2\times2\times2$) Monkhorst-Pack grid is used. Gaussian broadening is used with a width of 0.02 eV to smear the density of states. This combination of computational parameters ensures the convergence of total energies to within 5 meV/at. The atomic positions are relaxed until the Hellmann-Feynman force on each atom is reduced to within 0.05 eV/Å. The computed equilibrium lattice parameters of $TiO_2$ are 4.572 and 2.926 Å for *a* and *c* axes, respectively. On the other hand, the lattice information on monoclinic $HfO_2$ is as follows: $a=5.051$ Å, $b=5.175$ Å, $c=5.354$ Å, and $\beta=98.81°$. These computed values agree well with extant theoretical as well as experimental data.[11–13] The calculated energy gaps for $TiO_2$ and $HfO_2$ are 1.7 and 3.6 eV, respectively, to be compared with experimental data of 3.0 ($TiO_2$) (Ref. 14) and 5.66 eV ($HfO_2$).[15] The underestimation of the energy gap by 40% is typical for local density approximations.

We first present computational results on an isolated cation vacancy. We recall that all cations in rutile $TiO_2$ or

[a)]Author to whom correspondence should be addressed; electronic mail: hansw@ewha.ac.kr

 

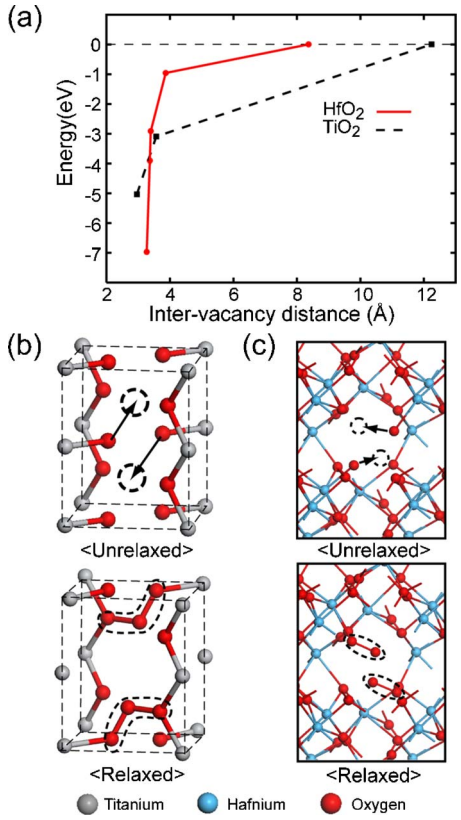


FIG. 1. (Color online) (a) interaction energy between cation vacancies with respect to the intervacancy distance. The reference values are the energies for largest separations. The atomic arrangements around most stable divacanices in $TiO_2$ and $HfO_2$ are shown in (b) and (c), respectively. For comparison, the initial configurations before relaxation are also displayed in the upper figures. The dashed circles indicate the cation vacancy sites.

monoclinic $HfO_2$ are equivalent by symmetry. The relaxation patterns in both materials are similar; when the cation is removed, oxygen atoms around the defect site relax outwards. In $TiO_2$, the atomic displacement is 0.05–0.1 Å, while oxygen atoms surrounding the Hf vacancy move outwards by 0.05–0.28 Å. In contrast with the oxygen vacancy where the electron carriers are induced[1] or in-gap states are developed,[2] the cation vacancy leads to a hole doping with two carriers per vacancy. That is to say, both Ti and Hf single vacancies do not induce pronounced gap states. On the other hand, it was reported that the Hf vacancy gives rise to the ferromagnetism. This is also confirmed in our calculation and the magnetic moment is found to be $3.3\mu_B$ per supercell, which is a value close to the previous calculation.[4] The spin density is largest at oxygen atoms around the missing Hf atom with local magnetic moments of $0.1\mu_B$–$0.5\mu_B$.

Next we consider the interactions between cation vacancies. One can choose various configurations within the given supercell. The computed interaction energies for closely separated cases are shown in Fig. 1. As a reference, the energy is evaluated for defects at the largest separation allowed for the given supercell. It is noticeable that energies at small separations are significantly lower than the reference values, with interaction energies as much as 5 or 7 eV per pair. In Figs. 1(b) and 1(c), the vacancy pair at the most stable configurations is shown for $TiO_2$ and $HfO_2$, respectively. The initial configurations before relaxation are also displayed to show the relaxation path more clearly. The removal of two cations (dashed circles) leaves the "dangling" oxygen atoms with only one metal-oxygen bonding. Note that these oxygen atoms were three-fold coordinated originally. Due to the unstable bonding, the oxygen atoms undergo large relaxation along the direction indicated by arrows in the upper figures. This results in the formation O–O bonding between the dangling oxygen and nearby oxygen atoms that were also undercoordinated. (See dashed curves in the lower figures.) The bond lengths between two oxygen atoms are 1.4–1.5 Å, in comparison with 1.21 and 1.27 Å for $O_2$ and $O_3$ molecules, respectively. In the case of $HfO_2$, there exist many combinations of two Hf vacancies in close separations. We find that the large relaxation is found only when removed cations were originally connected through three-fold coordinated oxygen atoms.

In Fig. 2, the densities of states (DOSs) are shown for $TiO_2$ and $HfO_2$ in bulk or with two cation vacancies. When two defects are far away, DOS is a simple sum of those for single vacancies (not shown). However, for clustered divacancies, strongly localized states appear in the energy gap. In the case of $TiO_2$, there are doubly degenerate levels at 0.5 eV above the valence top and they are fully occupied with four electrons. The distribution of wave functions indicates that they are mainly O $p$ orbitals which are originated from the clusters resembling $O_3$ molecules. [See the right

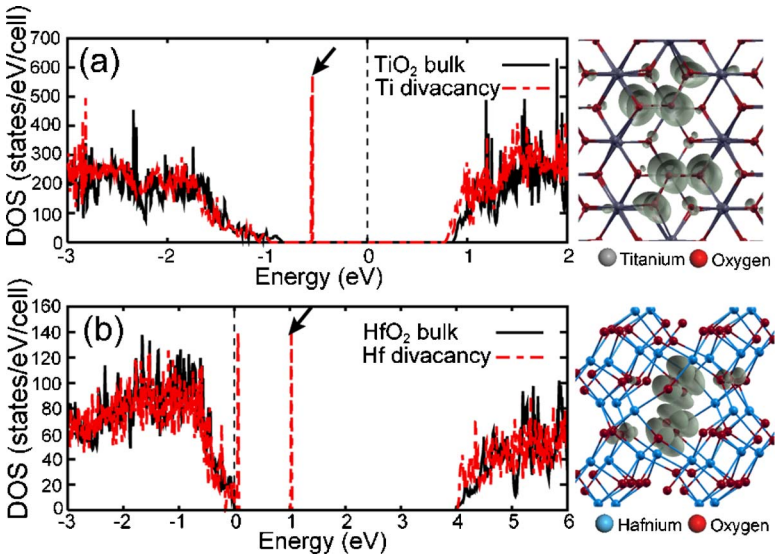


FIG. 2. (Color online) Density of states (DOS) for perfect the bulk and the supercell including divacancies in (a) $TiO_2$ and (b) $HfO_2$. The Fermi level is set to zero for all cases. The charge distribution for localized states indicated by arrows are shown on the right side. The character of O $p$ orbital is clearly visible.

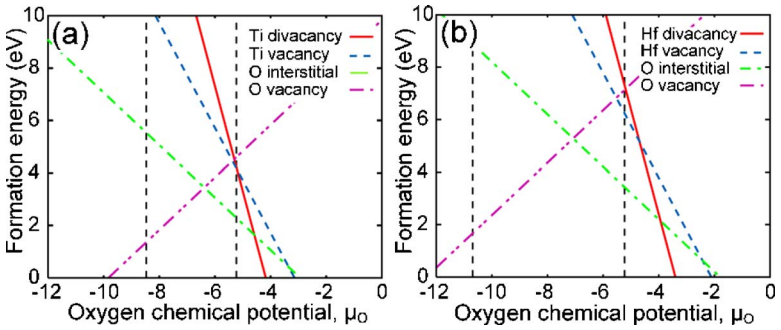


FIG. 3. (Color online) Defect formation energies of various point defects in (a) $TiO_2$ and (b) $HfO_2$. The dashed lines correspond to the metal- or oxygen-rich limits.

figure in Fig. 2(a).] The nodal structures between O $p$ orbitals are indicative of an antibonding character, i.e., $pp\pi^*$. The molecular states with bonding characters are much lower in energy and lie below the bottom of valence bands. On the other hand, there are two defect levels developed inside the energy gap of $HfO_2$ but they are unoccupied. [See Fig. 2(b).] This means that the cation divacancy in $TiO_2$ acts as a hole trap, while that in $HfO_2$ behaves like an electron trap site. We note that the relaxed structure of $TiO_2$ divacancy has a symmetric oxygen-bonding configuration leading to the degeneracy of in-gap states but the symmetry is lifted in the monoclinic $HfO_2$, splitting the energy level of defect states.

The presence of localized states could influence transport properties such as leakage currents or may increase the fixed charges that affect the threshold voltage shift. Near the oxygen-rich limit of the growth condition, the density of cation vacancy or oxygen interstitial will increase. We find that the oxygen interstitial gives rise to occupied shallow states close to the valence edge both for $TiO_2$ and $HfO_2$. Therefore, their impacts on the leakage currents will be less important than those of cation divacancies. In passing, the magnetic properties of $HfO_2$ are examined in the presence of the most stable divacancy. We find that the ferromagnetism in $HfO_2$ is mostly quenched in the paired vacancy; $O_2$ molecular units around Hf vacancies [dashed curves in Fig. 1(c)] possess a local momentum of only $\pm 0.23\mu_B$ with opposite signs between the units. That is to say, the ferromagnetic property of isolated cation vacancy will change to antiferromagnetic one after the formation of divacancy.

Lastly, we examine the defect formation energy of neutral point defects in $TiO_2$ and $HfO_2$ with respect to the chemical potential of the oxygen atom ($\mu_O$). (We refer to Ref. 1 for a detailed formulation.) The results are shown in Fig. 3. It is found that the oxygen vacancy or oxygen interstitial is energetically favorable for most range of $\mu_O$. Near the oxygen-rich side (upper limit of $\mu_O$), however, the formation energies of the oxygen vacancy and cation vacancy become comparable. On the other hand, the formation energy of the most stable cation divacancy is still higher than that of single vacancy over the entire range of oxygen chemical potential. This indicates that the cation divacancy is likely to be formed via migration and pairing of single cation vacancies.

This work was supported by the System IC2010 program of the Korean government, the Korea Science and Engineering Foundation through the Basic Research program (Grant No. R01-2006-000-10883-0). The computations were carried out at KISTI through the Strategic Supercomputing Program.

[1] E. Cho, S. Han, H.-S. Ahn, K.-R. Lee, S. K. Kim, and C. S. Hwang, Phys. Rev. B **73**, 193202 (2006), and references therein.
[2] A. S. Foster, F. Lopez Gejo, A. L. Shluger, and R. M. Nieminen, Phys. Rev. B **65**, 174117 (2002), and references therein.
[3] M. Venkatesan, C. B. Fitzgerald, and J. M. D. Coey, Nature (London) **430**, 630 (2004).
[4] C. D. Pemmaraju and S. Sanvito, Phys. Rev. Lett. **94**, 217205 (2005).
[5] J. Park, M. Cho, S. K. Kim, T. Park, S. W. Lee, S. H. Hong, and C. S. Hwang, Appl. Phys. Lett. **86**, 112907 (2005).
[6] S. K. Kim, S. Y. Lee, M. Seo, G.-J. Choi, and C. S. Hwang (to be published).
[7] E. San Andrés, M. Toledano-Luque, A. del Prado, M. A. Navacerrada, I. Mártil, G. González-Díaz, W. Bohne, J. Röhrich, and E. Strub, J. Vac. Sci. Technol. A **23**, 1523 (2005).
[8] G. Kresse and J. Hafner, Phys. Rev. B **47**, 558(R) (1993); **49**, 14251 (1994).
[9] P. E. Blöchl, Phys. Rev. B **50**, 17953 (1994).
[10] D. M. Ceperley and B. J. Alder, Phys. Rev. Lett. **45**, 566 (1980).
[11] X. Zhao and D. Vanderbilt, Phys. Rev. B **65**, 233106 (2002).
[12] A. A. Demkov, Phys. Status Solidi B **226**, 57 (2001).
[13] K. M. Glassford and J. R. Chelikowsky, Phys. Rev. B **46**, 1284 (1992).
[14] J. Pascual, J. Camassel, and H. Mathieu, Phys. Rev. B **18**, 5606 (1978).
[15] M. Balog, M. Schieber, M. Michman, and S. Patai, Thin Solid Films **41**, 247 (1977).